

Contents lists available at ScienceDirect

Engineering Fracture Mechanics

journal homepage: www.elsevier.com/locate/engfracmech





Accuracy of the predicting for creep-fatigue cyclic life based on parameters in a characteristic cycle

Biao Ding ^a, Weili Ren ^{a,*}, Yunbo Zhong ^{a,*}, Xiaotan Yuan ^a, Jianchao Peng ^b, Tianxiang Zheng ^a, Zhe Shen ^a, Yifeng Guo ^a, Weidong Xuan ^a, Jianbo Yu ^a, Josip Brnic ^c, Peter K. Liaw ^d

- a State Key Laboratory of Advanced Special Steel, College of Materials Science and Engineering, Shanghai University, Shanghai, PR China
- ^b Laboratory for Microstructures, Shanghai University, Shanghai, PR China
- ^c Faculty of Engineering, University of Rijeka, Vukovarska 58, Rijeka, Croatia
- ^d Department of Materials Science and Engineering, The University of Tennessee, Knoxville, USA

ARTICLE INFO

Keyword: Creep-fatigue Life prediction Characteristic cycle Linear damage summation Energy-life

ABSTRACT

The purposes of the present work are to evaluate the prediction accuracy of characteristic cycle on creep-fatigue life prediction and to analyze the advantages and disadvantages of various models in tensile strain-dwell tests. The parameters of the first cycle, the 10% life, the half-life, and the characteristic cycle that we proposed (a turning point between the initial rapid softening and subsequent slight softening/hardening) are employed to linear-damage-summation (LDS) and energy-life prediction models based on the creep-fatigue data of directionally-solidified Nickelbased superalloy, DZ445, at 900 °C. It is found that the characteristic cycle parameters with clear physical significance have the highest life prediction accuracy. Moreover, the optimal critical value of fatigue and creep damage (the coordinate of the creep-fatigue envelope intersection) in the LDS is also determined. The prediction accuracy of creep damage based on the time-fraction, the simple ductility-exhaustion, and the strain-energy- density-exhaustion models is sequentially improved in the LDS rule. In the energy-life model, the life prediction accuracy based on damage mechanism and frequency correction is higher than the value without any correction. This investigation provides a new method of the parameter-selection for the creep-fatigue life prediction, which is accurate and convenient. It provides the theoretical-guidance for creep-fatigue life prediction in both laboratory experiment and actual components.

1. Introduction

With the development of high-temperature equipment in gas turbine, aero engine, thermal power, and nuclear power, their components usually suffer from the creep-fatigue interaction failures during start-up, operation, and shut-down process. Thus, the investigations of creep-fatigue behavior as well as the life-prediction becomes particularly important [1,2].

Researchers have been devoted to the development of fatigue-life prediction models [3,4]. The earliest research on the development of fatigue-life prediction models could be traced back to 1855. Wöhler [5] studied the stress-life curve of high-cycle fatigue and established the famous S - N curve (where S represents the stress while N represents the life cycles, respectively). In 1910, Basquin [6]

E-mail addresses: wlren@staff.shu.edu.cn (W. Ren), yunboz@staff.shu.edu.cn (Y. Zhong).

Corresponding authors.

```
Nomenclature
D_{\rm f}
            total fatigue damage (-)
            total creep damage (-)
D_c
            creep-fatigue cycles at a certain level of fatigue load (-)
n_i
N_{fi}
            cyclic life at a certain level of fatigue load (-)
            creep-fatigue rupture time at a certain level of creep load (h)
ti
            pure creep-rupture time at a certain level of creep load (h)
t_{rj}
d_{\rm f}
            fatigue damage at a single cycle (-)
            creep damage at a single cycle (-)
d_c
(\overline{D_f}, \overline{D_c})
            coordinate of intersection between the creep-fatigue failure envelopes (-)
            fitting constant (-)
b
            fitting constant (-)
            fitting constant (-)
c
t_R(\sigma, T)
            function of the applied stress at a constant temperature (h)
            related constant of material and temperature (-)
α
            related constant of material and temperature (-)
N_f^p
            predicted life (-)
N_f^m
            measured life (-)
            number of data points (-)
n
\hat{I}\mu_{in}
            inelastic strain rate (%)
            elastic modulus (GPa)
Ε
\hat{I}((\hat{I}\mu_{\bar{i}n}, T_{abs})) ultimate creep strain (%)
Ε
            elastic modulus (MPa)
            inelastic-strain energy density rate (MJ/m^3 s^{-1})
\dot{w_{in}}
            inelastic strain energy density (MJ/m<sup>3</sup>)
Wf
            inelastic tensile strain energy (MJ/m<sup>3</sup>)
Wt
            failure reversals (-)
2N_{\rm f}
n′
            cyclic strain-hardening index (-)
            maximum tensile stress (MPa)
\sigma_{T}
\Delta \epsilon_{in}
            inelastic strain (%)
            constant (-)
R^2
            coefficient of determination (-)
T_c
            time in pure low-cycle fatigue (s)
            inelastic strain range (%)
\Delta \hat{I} \mu_{in}
\Delta \hat{I} \mu_{pp}
            plastic strain range (%)
            creep strain range (%)
\Delta I \mu_{cp}
            relaxed stress (MPa)
\Delta \sigma_{\rm r}
            creep strain range component (%)
\Delta I \mu_{cp}
```

described the stress-life data in the form of power-law for the first time. In the 1950s, Coffin [7] and Manson [8] independently reported the strain-life relationship in the low-cycle fatigue, namely, the famous Masson-Coffin formula, which initiated the study of creep-fatigue life-prediction models. Over the past 60 years, the creep-fatigue life-prediction models have been extensively developed, among which Halford [9], Chen [10], Korsunsky [11], Sabour [12], Takahashi [13], Yuan [14], Zhang [15,16], Wong [17], and others successively reviewed the creep-fatigue life-prediction methods of different system materials. Researchers have developed hundreds of creep-fatigue life-prediction models [18]. However, with the development of those models, the linear-damage-summation (LDS) rule could better predict the fatigue life and meet the requirements of remaining-life assessment [19]. Researchers usually use the traditional parameter methods to calculate the fatigue damage in LDS model [20]. In LDS model, the creep damage is usually calculated by the time-fraction (TF) method, the simple ductility-exhaustion (DE) method [21] as well as its evolution [22], and the strain-energy-density-exhaustion (SEDE) [23]. The energy-based life models not only consider the effects of temperature and total strain amplitude, but also the effects of internal defects, such as carbides and micro-voids, on the fatigue life [24]. It could combine the accuracy of life prediction with clear physical mechanisms [25,26].

The calculations of creep-fatigue damage in the above-mentioned life-prediction models require the parameters, such as stress, strain, and strain energy, which are required by the addition of damage cycle-by-cycle. Nevertheless, the cyclic-life in the creep-fatigue experiment is usually from hundreds to thousands or even tens of thousands of cycles in fact. It is obviously impractical to calculate the damage cycle-by-cycle. Therefore, some approximate values of the damage calculations are required. But the selection of parameters in different cycles is a very controversial issue in creep-fatigue deformation, which is directly related to the prediction accuracy.

Campbell calculated the creep-fatigue damage under the mid-life cycle for the 304 stainless steel at 650 °C with different strain-ranges, assuming that the total-damage is equal to the product of the damage (including the relaxation history, the maximum stress, the strain range, and the creep damage during dwell period) at 1/2 N_f and the cyclic-life. Since the cyclic-stress remains stable with 1.0% total strain-range at 650 °C in Campbell's research with tensile-dwell period, so this damage-calculation method should be effective [27]. This kind of calculation criterion is considered reasonable in the stress stability-state during deformation, such as for the creep-fatigue deformation of 709 Alloy [28]. However, with the appearance of cyclic softening/hardening in the deformation of most materials, the damage at the mid-life may not accurately represent the entire deformation behavior [28,29]. Therefore, some scholars select several representative cycles to calculate the total creep-fatigue damage for high prediction precision [30]. In order to balance the prediction accuracy and convenience of the creep-damage calculation, Chen [31] uses the parameter at every 10% creep-fatigue life as the representative damage to predict the life of Alloy 617 and HAYNES 230 alloy. The prediction showed the promising results as the difference between the predicted and experimental creep-fatigue life of Inconel 617 and Haynes 230 is less than 30% in the frequencymodified tensile hysteresis-energy model. However, in the first cycle during deformation, the calculated damage is much smaller than the value calculated based on the parameters at the half-life cycle [32]. In the creep-fatigue deformation of 9Cr-0.5Mo-1.8W-V-Nb heat-resistant steel, the parameter value under the first-cycle also shows more damage of stress relaxation compared with that in the half-life cycle [33]. Therefore, the predicted life using the parameters under the first cycle will lead to the large value. The concept of the cycle-by-cycle damage calculation is used in the creep-fatigue life prediction of GH4169 in a tensile-strain-dwell test with different total strain-ranges, which has good prediction accuracy within a scatter factor of 1.5 and can evaluate the remaining-life of material [32]. A new numerical procedure based on a cycle-by-cycle analysis was constructed for creep-fatigue behavior and life prediction of high-temperature structures under multi-axial stress states [34]. In general, the accuracy of life prediction cycle-by-cycle is the best. Certain creep-fatigue equipment [such as MTS (Mechanical Testing & Simulation Co., Ltd., Minnesota, U.S.A.), etc.] can record the plastic-strain and other parameters in each cycle directly. However, for some equipment [such as the RPL series (Changchun Research Institute for Mechanical Science Co., Ltd., Changchun, C.N.), etc.] that cannot record these parameters cycle-by-cycle, resulting in the calculation of damage for each cycle is extremely cumbersome [35]. Therefore, it is particularly important to select the convenient and accurate parameters during deformation to estimate the damage.

Our research suggests the use of parameters in the "characteristic cycle" to predict the life. The characteristic cycle is defined as the "turning point" between the initial rapid-softening and the subsequent slight-softening/hardening of the maximum tensile stress, which represents the transition from the unstable-state (the rapid generation of dislocations) to the steady-state (the dynamic equilibrium of the generation and annihilation of dislocations) during deformation [Fig. 4 (a) for details]. It could reflect the deformation behavior of material throughout the entire process. In order to evaluate its impact on the accuracy of the life-prediction, based on the creep-fatigue data of the DZ445 superalloy under different total strain ranges and dwell times at 900 °C, we compared the prediction accuracy calculated by the parameters at the characteristic cycle, the first cycle, the 10%-life, and the half-life. The linear-damage-summation and energy-life models are employed to evaluate their accuracy. The calculation of fatigue and creep damage are required in the LDS. The traditional parametric methods are used to calculate the fatigue damage. The time-fraction, the simple-ductility-exhaustion, and the strain-energy-density-exhaustion models are employed to calculate the creep damage. The results show that the creep-fatigue life prediction using the parameters under the characteristic cycle has good accuracy. This research work provides a new method of parameter selection in life prediction. This kind of prediction method is accurate and convenient, which provides the guidance for creep-fatigue life-prediction of the experiment both in laboratory and practical components.

2. Experimental process and flow chart of life-prediction

2.1. Experimental process

The main chemical composition of the first-generation directionally-solidified Nickel-based superalloy, DZ445, selected in this investigation is: 0.072 C, 13.10 Cr, 9.99 Co, 4.53 W, 1.75 Mo, 4.07 Al, 2.38 Ti, 4.80 Ta, 0.024 B, and Ni is the balance (Weight percentage, %). The detailed microstructure of this superalloy could be found in our previous investigation [36]. All the strain-controlled creep-fatigue experiments were performed on the RPL series electronic creep-fatigue testing machine (RPL is a testing machine model, produced by Changchun Research Institute for Mechanical Science Co., Ltd., Changchun, C.N.). The strain loading/unloading rate keeps a constant at $5 \times 10^{-3} \, \text{s}^{-1}$ with or without dwell time. Different dwell times are introduced at the maximum tensile-strain of the triangular-wave to form a trapezoidal-wave. The strain ratio, R (R = $\hat{\mu}_{min}/\hat{\mu}_{max}$) is -1. Other detailed experimental processes could be seen in our previous study [37]. The data used in the creep-fatigue life prediction of this investigation are shown in Table 1. Each set of the experiments is repeated 2–3 times until the sample is broken. The fracture position is regarded as an effective fracture within the range of the gauge length. The creep-fatigue life is defined as the number of cycles (N_f) when the sample is broken.

Table 1
Creep-fatigue experiment parameters at 900 °C for the DZ445 superalloy.

Temperature (°C)	Strain (%)	Dwell time (min.)
900	0.6	0, 2, 3, 5, 8
	1.0	0, 2, 3, 8
	1.6	0, 2, 3, 5, 8,

2.2. Overall flow chart of life prediction

The overall flow chart used to predict the creep-fatigue life of DZ445 superalloy in our investigation is shown in Fig. 1. The first purpose of our study is to determine which cycle parameter selected as the reference damage has the highest life prediction accuracy? The second purpose is to determine which the optimal model is by comparing the life prediction accuracy of different models. We select the parameters at the first cycle, the 10% life, the half-life, and the characteristic cycle to predict the life in the LDS and energy-life model. In the linear-damage-accumulation rule, we aim to determine the optimal intersection coordinates in the creep-fatigue envelope first. Then we calculate the fatigue-damage and creep-damage separately. In the creep-damage calculation, we select the time fraction, the simple ductility-exhaustion, and the strain-energy-density exhaustion rules, respectively. In the energy-life model, we select the uncorrected model, the damage-mechanism-modified model and the frequency-modified model, respectively. Finally, the accuracy of the life prediction model is calculated by the deviation between the predicted life and the measured life. So as to determine which cycle parameter selected and which life-prediction model has the best prediction accuracy. The corresponding calculation method of life-prediction will be introduced in detail below.

3. Evaluation using a linear-damage-summation (LDS) model

3.1. Description of the LDS model

The time-independent fatigue damage and time-dependent creep damage are simply added in the linear-damage-summation model [38],

$$D_f + D_c = \sum \frac{n_i}{N_{f_i}} + \sum \frac{t_j}{t_{r_j}} = 1$$
 (1)

where D_f , D_c , n_i , N_{fi} , t_j , and t_{rj} stand for the total fatigue damage, the total creep damage, the cycles at a certain level of fatigue load, the corresponding cyclic life, the rupture time at a certain level of creep load, and the corresponding creep rupture time, respectively.

In the creep-fatigue interaction deformation, when the summation of fatigue and creep damage reaches the set critical value, the material failure is considered to occur. In the case of the failure criterion for the bilinear relationship in the creep-fatigue interaction diagram (Fig. 2), the creep-fatigue cyclic life could be estimated by the following formula [24],

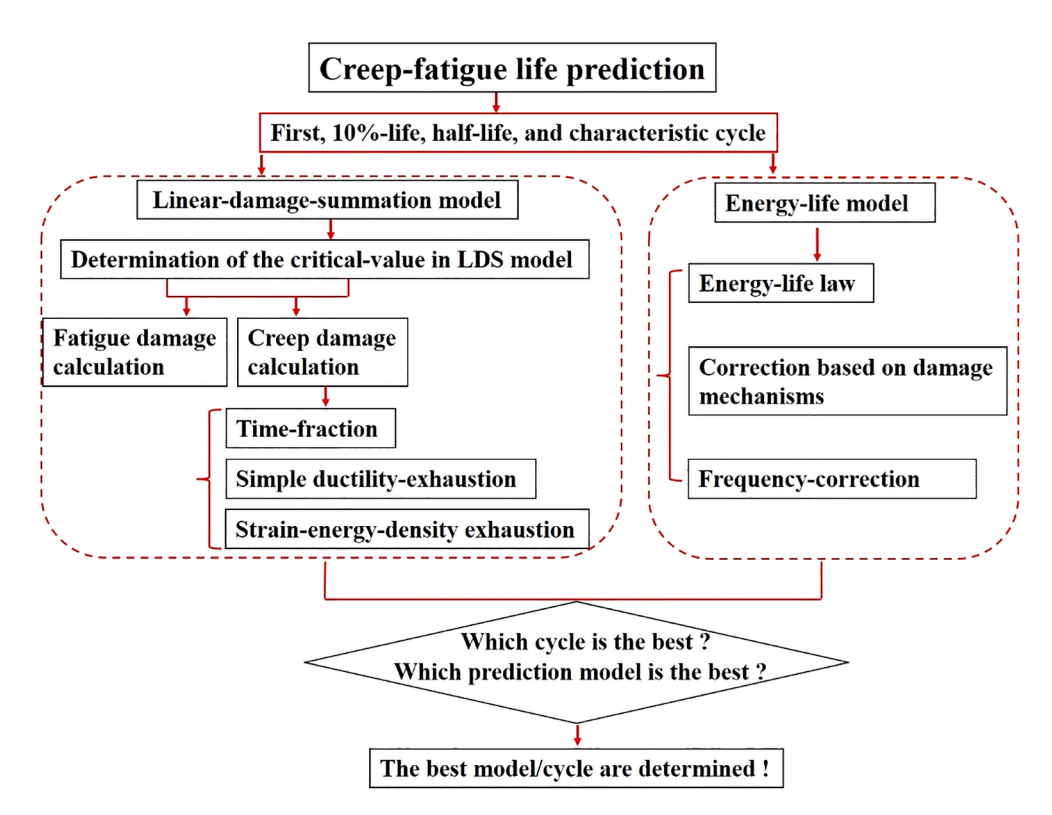


Fig. 1. Step-by-step image of the experiments and the life prediction.

$$N_{c-f} = \frac{\overline{D_c}}{\left(1 - \overline{D_f}\right) d_c + \overline{D_c}} d_f \left(if d_f / d_c \ge \overline{D_f} / \overline{D_c} \right)$$
(2)

$$N_{c-f} = \frac{\overline{D_f}}{\left(1 - \overline{D_c}\right) d_f + \overline{D_f}} d_c \left(if d_f / d_c < \overline{D_f} / \overline{D_c}\right)$$
(3)

where d_f and d_c represent fatigue and creep damage at a single cycle, respectively. The $\overline{D_f}$ and $\overline{D_c}$ are the coordinates of intersections between the two failure envelopes.

For the creep-fatigue design codes of different materials, the selection of intersection coordinates for the two failure envelopes is different. For example, the following values are used for the P91 steel in the current design code, $\overline{D_f} = 0.1$, $\overline{D_c} = 0.01[39]$; $\overline{D_f} = \overline{D_c} = 0.3$ [40]. The bilinear intersection of the "L" shape is defined as (0.1, 0.1) [41]. For other alloys, such as 304, 316, 316L, 316L(N), 316H, Alloy 800, and so on, the bilinear intersection in the RCC design rule is also set to (0.3, 0.3). For the $2\frac{1}{4}$ Cr1Mo steel and low-alloy ferritic steel, there is no available design rule currently [42]. Because the design rule for the DZ445 superalloy is also not clear yet, in order to obtain the optimal design criteria, the coordinates of the intersections for creep-fatigue failure envelopes as (0.5, 0.5), (0.3, 0.3), (0.1, 0.1), and (0.1, 0.01) are selected for life-prediction, respectively.

3.2. Determination of the critical-value in LDS model (intersection of the creep-fatigue envelope)

The determination of the critical value in linear-damage-summation requires the calculation of fatigue- and creep- damage, respectively. The traditional parametric methods are usually used to calculate the fatigue damage. The time-fraction, the simple-ductility-exhaustion, and the strain-energy-density-exhaustion models are employed to calculate the creep-damage.

3.2.1. Calculation of fatigue-damage

The fatigue-damage (d_f) of each cycle in creep-fatigue deformation could be simply estimated as the reciprocal of the cyclic life at the same $\Delta\epsilon_t$ and $\hat{I}\mu$ in pure-fatigue experiments [20], which could be expressed as a function of the total strain range $(\Delta\epsilon_t)$ in the Manson-Coffin form [43],

$$d_f = \frac{1}{N_f} = \frac{1}{a\Delta\varepsilon^{-b}} \tag{4}$$

where a and b are the fitting constants.

The pure fatigue test data and corresponding fitting results of the DZ445 superalloy with different total-strain-ranges at $900\,^{\circ}$ C are listed in Table 2 and Fig. 3, respectively. The functional relationship between the fatigue-damage and total-strain-range is,

$$d_f = \frac{1}{N_f} = \frac{1}{a\Delta\varepsilon_t^{-b}} = \frac{1}{1633.18\Delta\varepsilon_t^{(-4.97)}}$$
 (5)

3.2.2. Calculation of creep-damage

In the time-fractional model, the relationship between the creep damage (d_c) under the dwell time (t_h) in a single creep-fatigue cycle and the creep rupture time (t_R) under the equal stress conditions is:

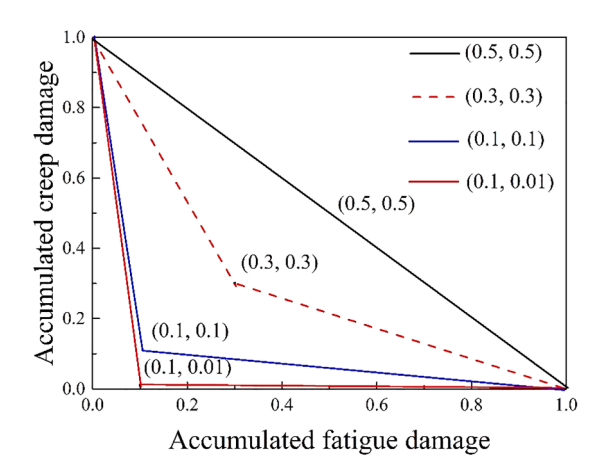


Fig. 2. Creep-fatigue interaction diagram in the linear-damage-summation rule.

Table 2 The pure fatigue experimental results with different total strain ranges at 900 $^{\circ}$ C for the DZ445 superalloy (Statistical results are the average value).

Total strain range (%)	Dwell time (min.)	Cyclic life (N_f)
0.6	0	20,681
1.0	0	1,552
1.6	0	595

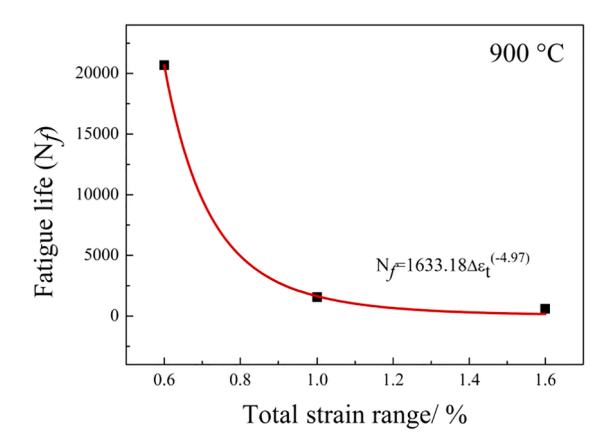


Fig. 3. Relationship between the total strain range and cyclic life at 900 °C for the DZ445 superalloy.

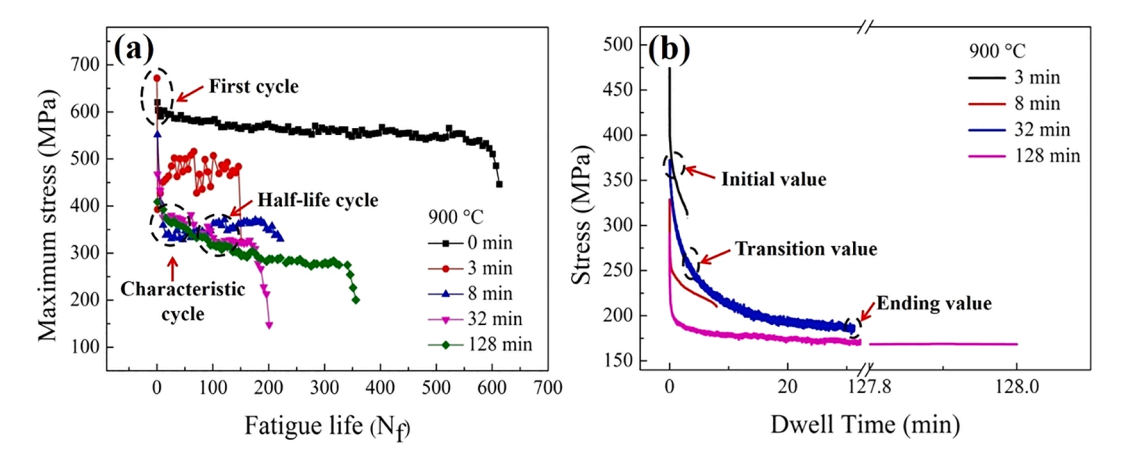


Fig. 4. Maximum tensile stress response with fatigue life (a) and stress-relaxation response with dwell time in a dwell-period at the characteristic cycle (b) of creep-fatigue tests for the DZ445 superalloy with a 1.6% total strain range at 900 °C.

Table 3 Experimental results of pure creep under different stress at 900 $^{\circ}$ C for the DZ445 superalloy.

Temperature/°C	Stress/MPa	Rupture time/h	Elongation /%
900	300	313	11.2
900	320	278	24.9
900	350	126	21.0
900	375	76	19.8

$$d_{c} = \frac{t_{i}}{t_{R}(\sigma_{i})} = \frac{t_{h}}{t_{R}} = \int_{0}^{t_{h}} \frac{dt}{t_{R}(\sigma, T)}$$
 (6)

where t_i represents the creep-rupture time under a stress, σ_i , and $t_R(\sigma, T)$ is a function of the applied stress at a constant temperature,

$$t_{R}(\sigma, T) = k \cdot \sigma^{-\alpha} \tag{7}$$

where k and α are the related constants of material and temperature. Some researchers use the initial value, the average value, the golden section value, or the ending value of the stress-relaxation stage as the reference stress in Eq. (6) to calculate the creep damage [Fig. 4(b)] [44]. In fact, the stress in the dwell-period is constantly relaxed. In order to accurately represent the stress, different expressions have been proposed to describe the stress relaxation behavior [24,45–47].

The pure-creep test results of the DZ445 superalloy under different stress levels at $900\,^{\circ}$ C are listed in Table 3. The stress and the corresponding rupture time are fitted in Fig. 5.

The creep-fatigue relaxation stress of the DZ445 superalloy at the characteristic cycle could be expressed as a function of the dwell time.

$$\sigma = a - b \ln(t + c) \tag{8}$$

where σ and t represent the stress and the time during the dwell period, respectively. The a, b, and c are the fitting parameters, whose values are listed in Table 4. Combining the above equations and data, the creep-damage expression in the time-fraction rule is,

$$d_c = \int_0^{t_h} \frac{dt}{t_R(\sigma,T)} = \int_0^{t_h} \frac{dt}{1020.93\sigma - 6.7025} = \int_0^{t_h} \frac{dt}{1020.93[a - b In(t+c)] - 6.7025} \tag{9}$$

3.2.3. Calculation of the optimal critical-value

In order to select the optimal design rule and cycle parameters, the coordinates of the intersections for the two failure envelopes as (0.5, 0.5), (0.3, 0.3), (0.1, 0.1), and (0.1, 0.01) were selected, respectively. Combined with the creep-fatigue data at the first cycle, the 10% life, the half-life, and the characteristic cycle of the DZ445 superalloy at 900 °C, Eq. (2) is employed to predict the creep-fatigue cyclic life. Since there are the same trends in the calculation results in different cycles, thus, only the results at a characteristic cycle would be analyzed as the representative. When the stress-integral value at a characteristic cycle is used as the reference damage, both the cyclic life predicted by the time-fraction method and the value measured are shown in Fig. 6. When the coordinates of the intersections of the two failure envelopes are (0.5, 0.5) and (0.3, 0.3), the predicted life is mostly high, and the overall predicted life deviation is within the 4 - times deviation band. When the coordinates are taken as (0.1, 0.01), the predicted life is basically low. The prediction accuracy is about 8 times deviation, whose accuracy is the worst. When the coordinate is (0.1, 0.1), the life prediction accuracy is the highest, which is within the deviation band of 3 - times.

The above results indicate that for the prediction of the creep-fatigue cyclic life of the DZ445 superalloy at 900 $^{\circ}$ C, the design rule for choosing the coordinate of (0.1, 0.1) has the highest life accuracy. Therefore, when using the LDS method to predict the cyclic-life in this investigation, we all choose the design rule that the intersection of the two failure envelopes is (0.1, 0.1).

3.3. Evaluation criteria of life prediction accuracy

The ability of a life prediction model is usually determined by standard deviation (SD), which indicates the degree to which a group of data is close to the average value. The smaller value represents the better life prediction ability of the model. The standard deviation is defined as follows [48]:

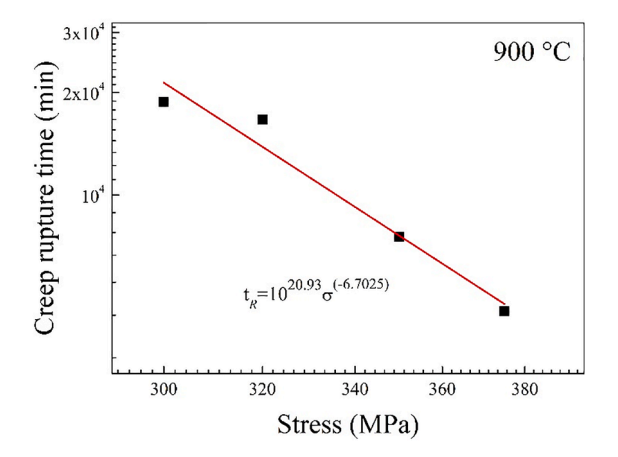


Fig. 5. Relationship between the applied-stress and the creep-rupture time (unit, minute) at 900 $^{\circ}$ C for the DZ445 superalloy.

Table 4
Stress-relaxation fitting parameters in a dwell period under different creep-fatigue test conditions for the DZ445 superalloy at 900 °C.

ε _t (%)	T _h (min.)	a	b	c
0.6	2	151.37	1.72	-0.02
0.6	3	153.74	0.88	-0.01
0.6	5	140.34	1.57	-0.01
0.6	8	101.49	1.69	0.01
1.0	2	191.98	7.27	-0.01
1.0	3	192.47	4.31	-0.07
1.0	8	194.15	2.01	-0.07
1.6	2	256.91	15.91	-0.01
1.6	3	349.32	27.75	0.08
1.6	5	259.05	13.57	0.01
1.6	8	240.95	11.96	0.01
1.6	16	230.45	12.54	0.02
1.6	32	225.34	13.54	-0.01
1.6	64	207.89	11.45	0.01
1.6	128	201.98	10.34	0.02

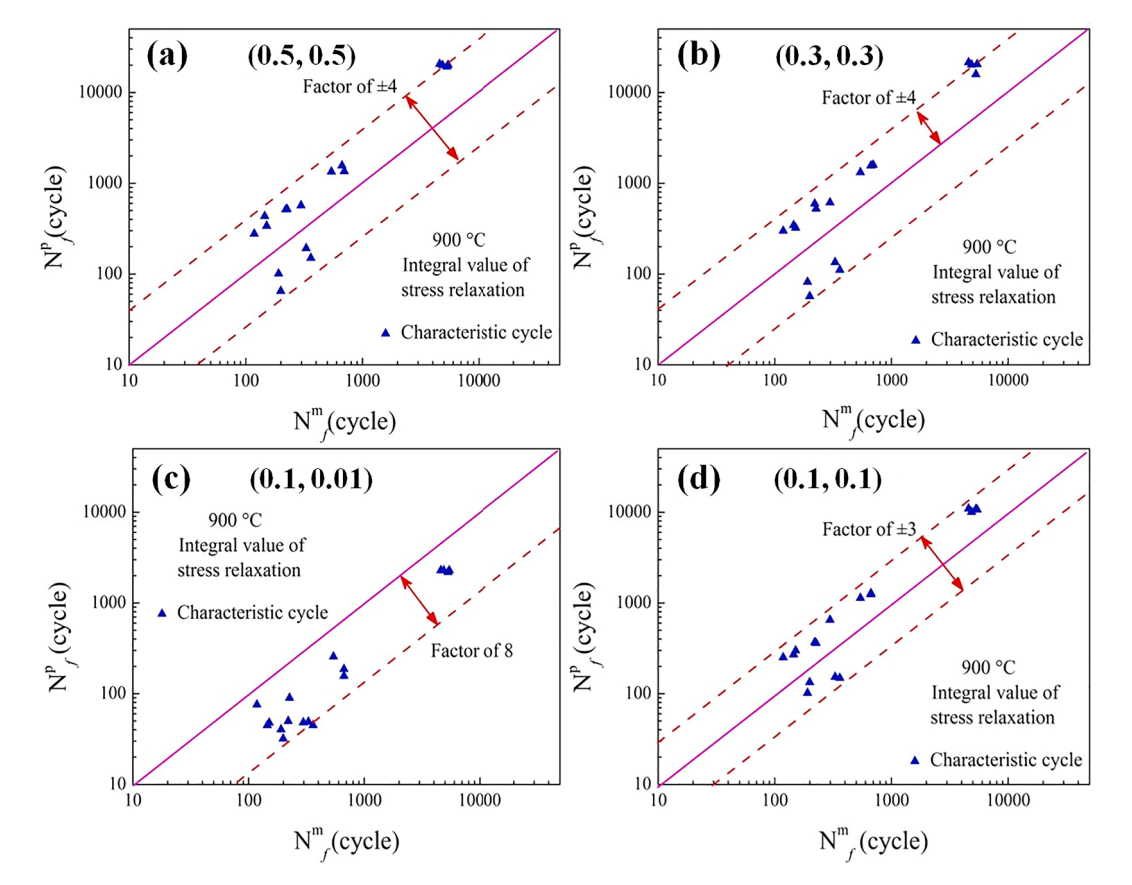


Fig. 6. Predicted cyclic life (N_f^p) and measured cyclic life (N_f^m) for DZ445 superalloy at 900 °C using a time-fraction method under integral stress values at a characteristic cycle with different design rules.

$$SD = \left[\frac{\sum_{1}^{n} (\lg N_f^p - N_f^m)^2}{n - 1} \right]^{1/2}$$
 (10)

where N_p^p , N_n^m , and n represent the predicted life, the measured life, and the number of data points, respectively.

3.4. Evaluation of the creep-damage in LDS using the time-fraction method

Based on the stress-integral value at the dwell-period under different cycles as the reference damage, the predicted life of creep-

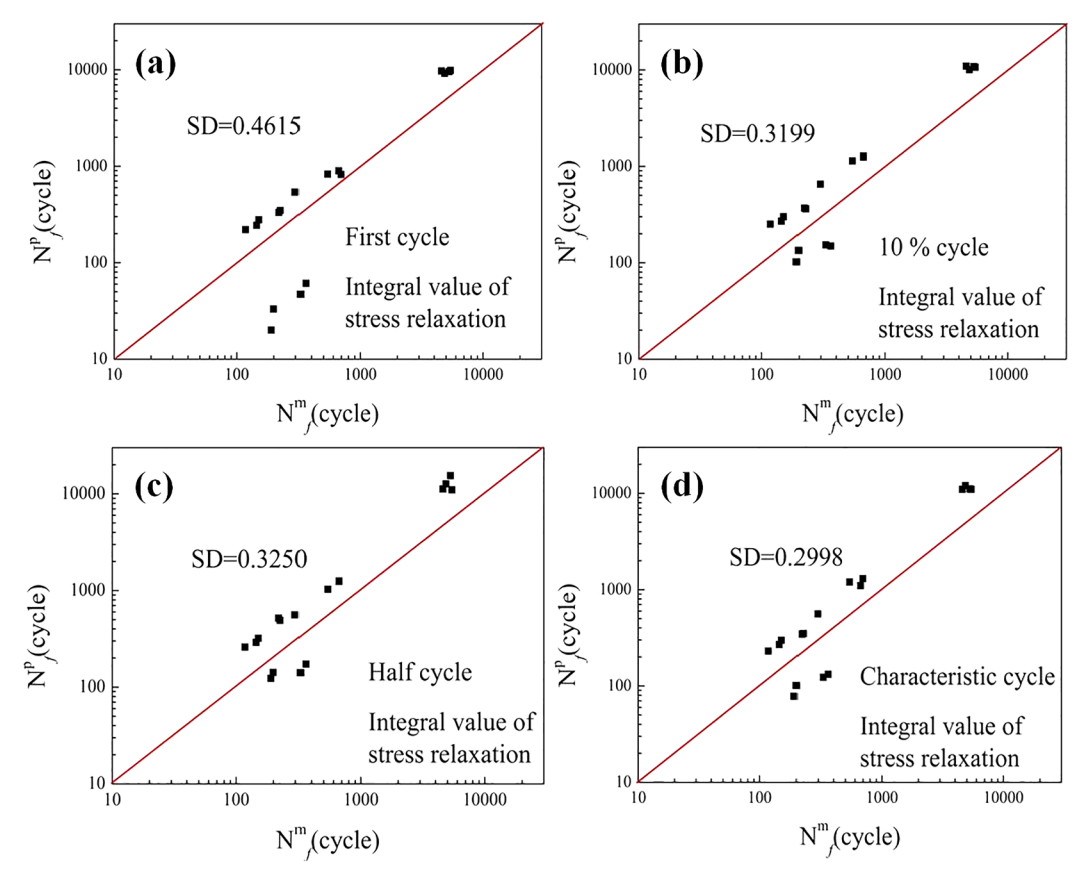


Fig. 7. Predicted cyclic life (N_f^p) and measured cyclic life (N_f^m) of the DZ445 superalloy at 900 °C using the time-fraction method under stress-relaxation integral values at different cycles. (a) The first; (b) the 10%; (c) the half-life; (d) the characteristic cycle.

damage calculated by the time-fraction method, the measured life and its standard deviations are shown in Fig. 7. The degree of correlation between the measured and predicted life in the selected characteristic cycle is the best with the SD of 0.2998 [Fig. 7(d)]. The prediction accuracy is the worst in the first cycle, with the SD of 0.4615 [Fig. 7(a)]. The prediction correlation between the values at 10% and half-life is slightly inferior to that in the characteristic cycle, with the SD of 0.3199 and 0.3250, respectively [Fig. 7(b) and (c)].

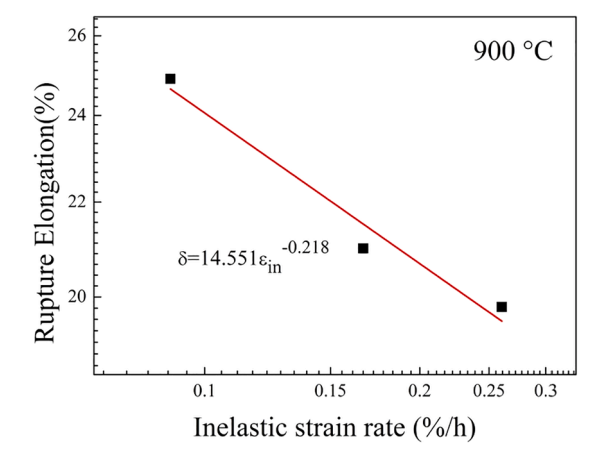


Fig. 8. Relationship between the inelastic-strain rate and the creep-rupture elongation under different stresses of the DZ445 superalloy at 900 °C.

3.5. Evaluation of the creep-damage in LDS using the simple ductility-exhaustion method

The relationship between the inelastic strain rate $(\hat{\mu}_{in})$ and the stress (σ) during the stress relaxation of the material is [49],

$$\varepsilon_{\rm in} = \frac{d\varepsilon_{\rm in}}{dt} = -\frac{1}{E} \frac{d\sigma}{dt} \tag{11}$$

where E is the elastic modulus. In the simple-ductility-exhaustion model, Goldhoff [50] and Oding [51] assume that the material has an ultimate creep strain, $\delta(\varepsilon_{\rm in}, T_{\rm abs})$, which is a function of strain rate and temperature. The rate of inelastic-strain is considered to be the main parameter for controlling the creep-damage [21], which has been replaced by the stress-integral-value expression in Section 3.1, the creep-damage at per cycle is simply expressed by:

$$d_{c} = \int_{0}^{t_{h}} \frac{\varepsilon_{in}}{\delta(\varepsilon_{in}, T_{abs})} dt = \int_{0}^{t_{h}} \frac{\frac{1}{E} \frac{b}{(t+c)}}{\delta(\varepsilon_{in}, T_{abs})} dt$$

$$(12)$$

where t_h and E are the dwell time of a single cycle and elastic modulus, respectively, and E \approx 94.7 GPa is for the DZ445 superalloy at 900 °C [52]. In the pure creep test, $\epsilon_{\rm in}$ is calculated by dividing the strain limit (δ) of the "enduring plasticity" by the rupture time. The relationship between them is approximately:

$$\delta = d \cdot \varepsilon_{in}^{\beta}$$
 (13)

The constants in the above models could be obtained by the data fitting or the creep tests at same temperature. The relationship between the inelastic-strain rate and the creep-strain limit as well as the corresponding fitting formula are presented in Fig. 8.

Combining the above data and Eq. (2), predicted and measured life of the DZ445 superalloy at 900 °C using a simple ductility-exhaustion method with different cycles are presented in Fig. 9. Compared with the life-prediction accuracy of using the time-fractional model (the prediction deviation is mostly within 3 times), the application of the simple ductile-exhaustion method has a higher prediction accuracy (within the deviation of 2 times). As shown in Fig. 9(a), the life predicted using the data at first cycle is larger than the measured life. Therefore, the predicted life is non-conservative. While as shown in Fig. 9(b-d), some predicted lives are

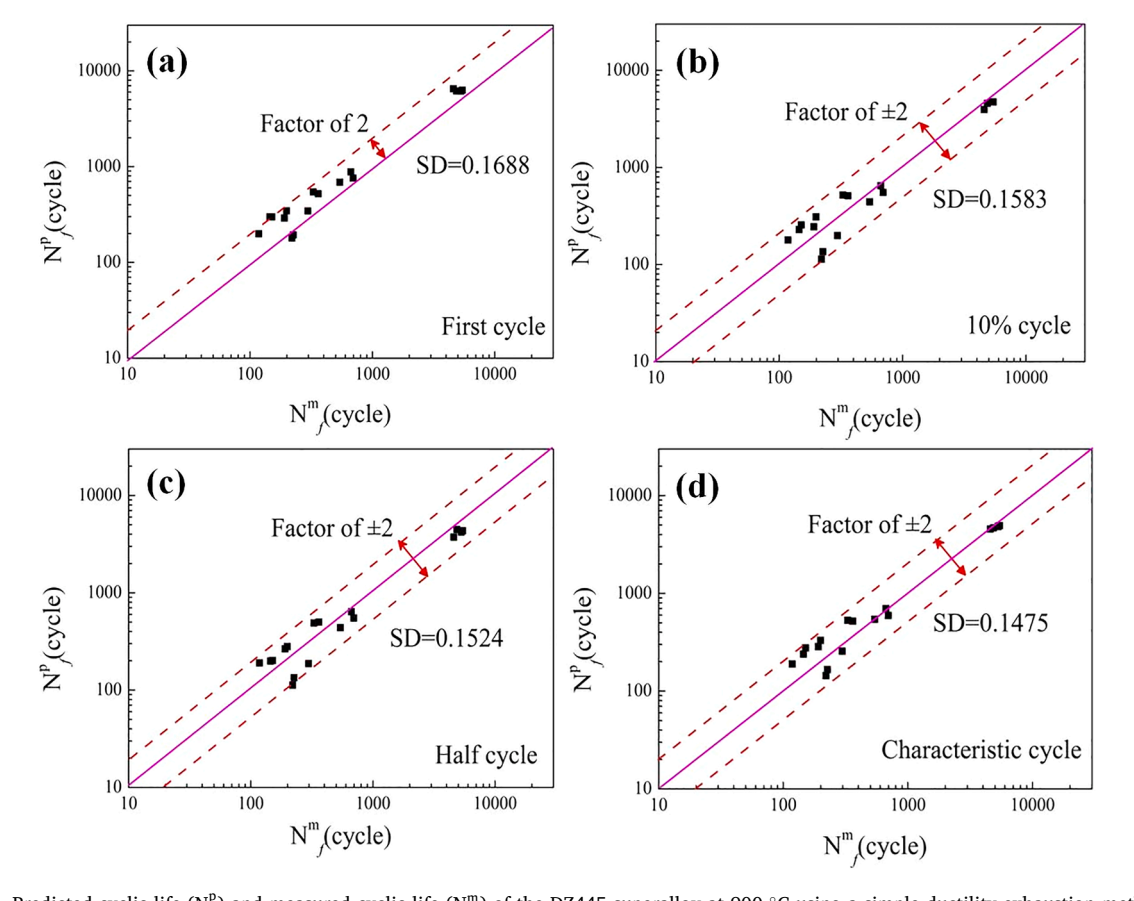


Fig. 9. Predicted cyclic life (N_f^p) and measured cyclic life (N_f^m) of the DZ445 superalloy at 900 °C using a simple ductility-exhaustion method at different cycles. (a) the first; (b) the 10% life; (c) the half-life; (d) the characteristic cycle.

larger/smaller than the measured life. Thus, the life predicted using the data at the 10% life, the half-life, and the characteristic cycle are distributed on both sides of the measured life line. This is because with the development of deformation, the plastic strain range at each cycle continues to increase [32,33]. Therefore, compared with the 10% life, the half-life, and the characteristic cycle, the plastic strain range under the first cycle is the smallest. Thus, the calculated inelastic strain rate is also the smallest with first cycle. The corresponding fracture elongation is large. Thus, the creep damage is small, resulting in the large predicted life. The Chaboche cyclic constitutive equation considering the time-recovery effect shows that with the increase of the fatigue life, the plastic deformation gradually increases and tends to be stable finally [53]. Therefore, the predicted lives calculated by using the parameters under 10% life, the half-life, and the characteristic cycle gradually decrease and are distributed on both sides of the actual measurement line.

Further analysis of Fig. 9 shows that the prediction accuracy is the highest under the selected characteristic cycle (the SD is 0.1475) [Fig. 9(d)], and the first cycle is the worst (the SD is 0.1688) [Fig. 9(a)]. The prediction accuracy of the 10% life and half-life is in the second place, with the SD of 0.1583 [Fig. 9(b)] and 0.1524 [Fig. 9(c)], respectively. It shows that when the simple ductility-exhaustion model is used to calculate the creep-damage in the LDS rule, and the life prediction accuracy is the highest when the characteristic cycle parameters are selected as the reference damage.

3.6. Evaluation of the creep-damage in LDS using the strain-energy-density exhaustion

In Fig. 8, the rupture elongation of the DZ445 superalloy at 900 °C may deviate from the inelastic-strain rate, and the corresponding mechanism of this behavior has not been clearly explained. Therefore, the rupture elongation may not be an ideal index of the material ductility. It may be a better choice to use the inelastic-strain energy of the comprehensive stress and strain factors as the parameter to control creep-fatigue damage. Combined with the stress relaxation, Eq. (8), the expression of creep-damage under a single creep-fatigue cycle in the SEDE model is:

$$d_{c} = \int_{0}^{t_{h}} \frac{\dot{W_{in}}}{W_{f}(\dot{W_{in}}, T_{abs})} dt = \int_{0}^{t_{h}} \frac{\sigma \cdot \dot{\varepsilon_{in}}}{\int_{0}^{t_{R}} \dot{W_{in}} dt} dt = \int_{0}^{t_{h}} \frac{\left[a - b In(t+c)\right] \cdot \frac{1}{E} \frac{b}{(t+c)}}{\sigma \cdot \delta} dt$$

$$(14)$$

where t_h , t_R , σ , and δ are the dwell time of a single cycle, the rupture time of the creep test, the stress level, and the elongation under the

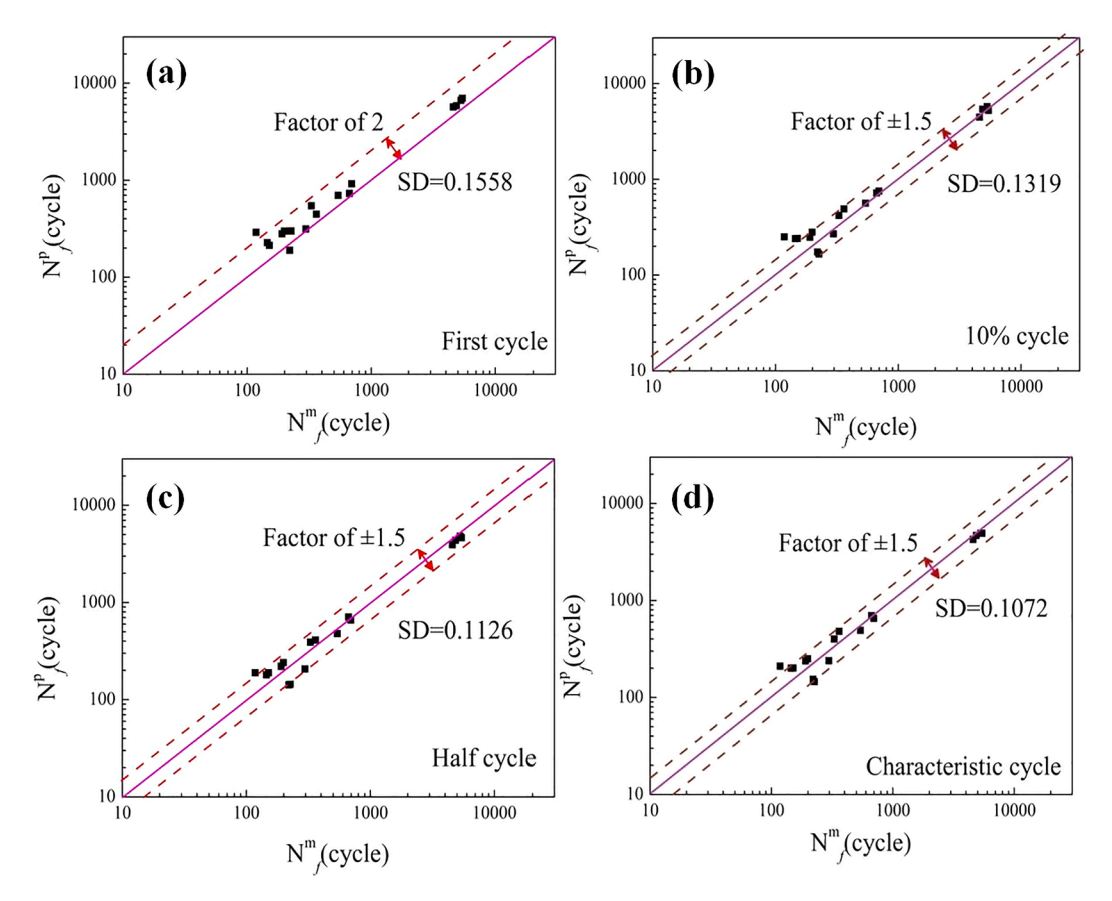


Fig. 10. Predicted cyclic life (N_p^p) and measured cyclic life (N_p^m) of the DZ445 superalloy at 900 °C using SEDE methods with different cycles. (a) the first; (b) the 10% life; (c) the half-life; (d) the characteristic cycle.

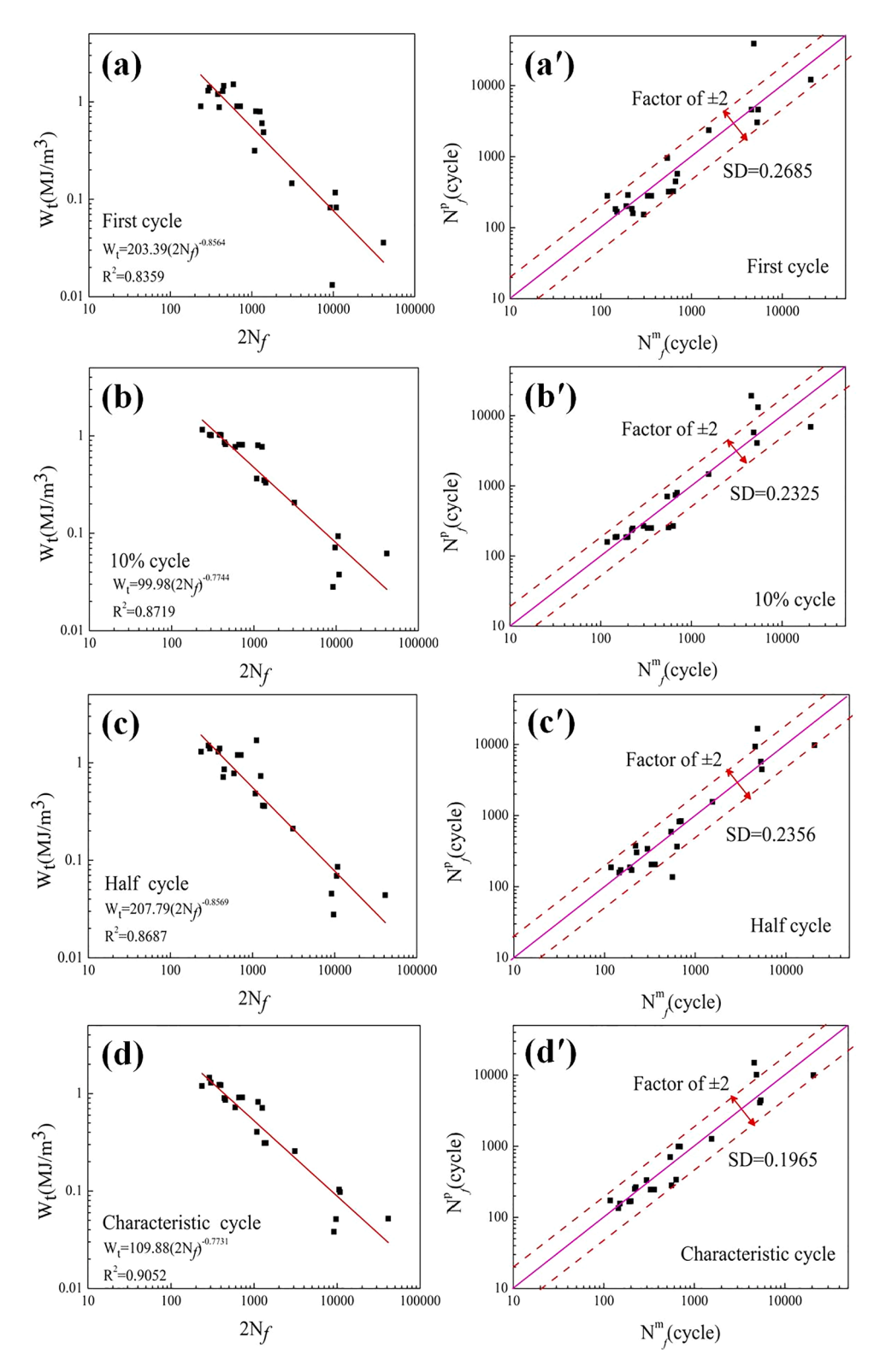


Fig. 11. The energy with different cycles as a function of cyclic life of creep-fatigue tests for the DZ445 superalloy at 900 °C and predicted cyclic life (N_f^p) as a function of the measured cyclic life (N_f^m) . (a and a') first; (b and b') 10%-life; (c and c') half-life; (d and d') characteristic cycle.

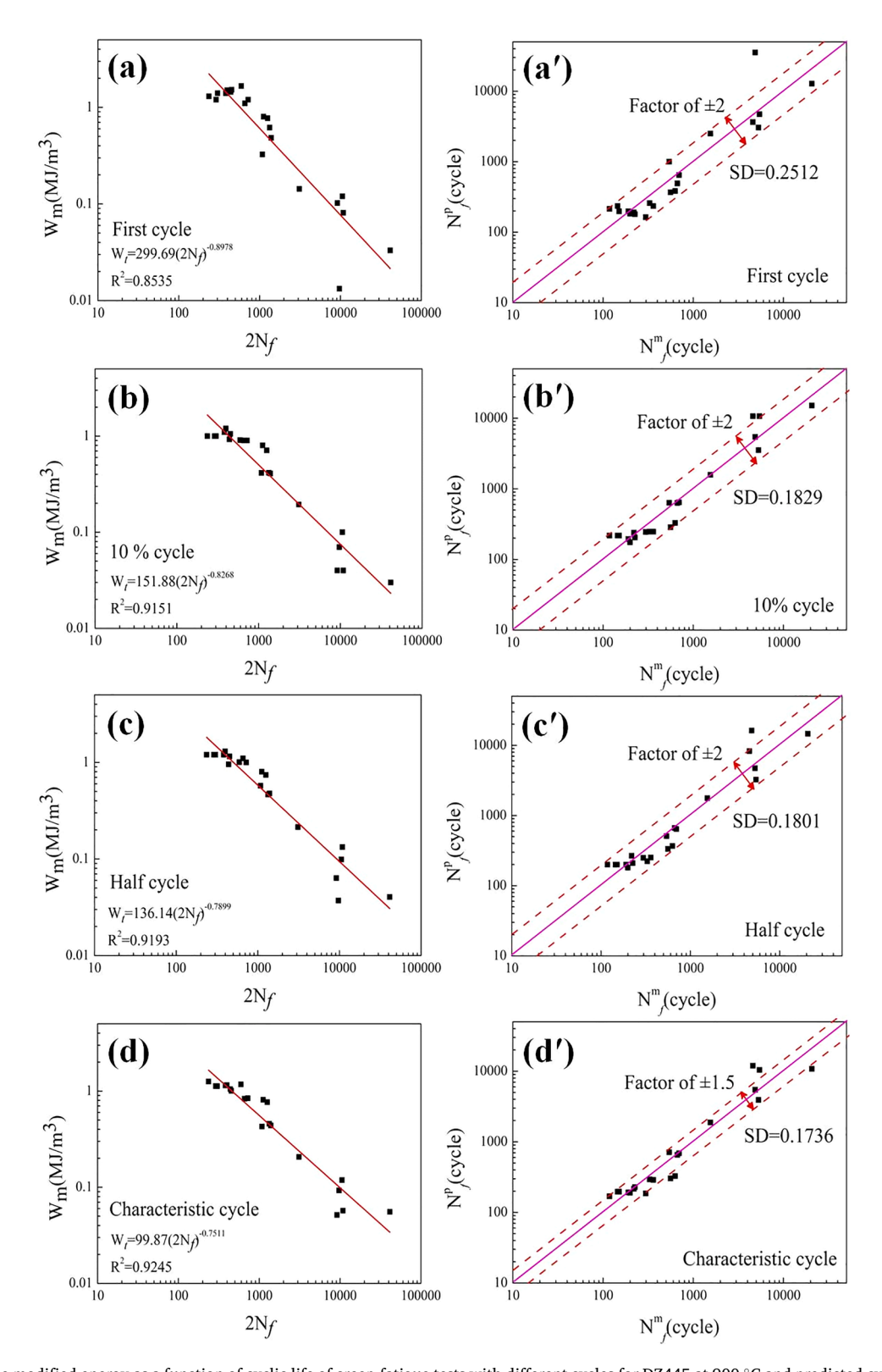


Fig. 12. The modified energy as a function of cyclic life of creep-fatigue tests with different cycles for DZ445 at 900 °C and predicted cyclic life (N_p^p) as a function of measured cyclic life (N_f^m) . (a and a') the first; (b and b') the 10%-life; (c and c') the half-life; (d and d') the characteristic cycle.

stress level, respectively. win is the inelastic-strain energy density rate,

$$\dot{\mathbf{w}}_{\mathrm{in}} = \boldsymbol{\sigma} \cdot \dot{\boldsymbol{\varepsilon}}_{\mathrm{in}}$$
 (15)

where w_f is the inelastic strain energy density accumulated to material failure,

$$\mathbf{w}_f = \int_0^{t_R} \mathbf{w}_{\text{in}} d\mathbf{t} = \sigma \cdot \delta \tag{16}$$

The constants in the above models could be obtained by the data fitting or the pure creep tests at the same temperature.

Combining the data in the above equations and Eq. (2), the relationship between the measured and the predicted lives using the SEDE model at different cycles are shown in Fig. 10. After applying the SEDE method, the overall prediction accuracy is relatively high (the prediction deviations of most data points are within ± 1.5 times). The cyclic life predicted by using the first-cycle data is slightly larger. While some data points in the predicted life using the data under 10% life, half-life, and characteristic cycle are conservative. This is because compared with the 10% life, the half-life, and the characteristic cycle, the plastic strain range under the first cycle is the smallest. Thus, the inelastic-strain energy consumed in the initial stage of creep-fatigue loading is small, and the calculated inelastic-strain energy-density rate is also small [32,33]. The corresponding creep-damage is too small, yielding a larger predicted life. With the development of deformation, the inelastic strain energy gradually increases and tends to be steady [32]. Thus, the corresponding creep damage is increased, which results in the decreased predicted life. Therefore, the data of predicted life is distributed on both sides of the measured life line.

The highest life-prediction accuracy (the SD is 0.1072) is present when the data at the characteristic cycle is used as the damage parameter [Fig. 10(d)]. The prediction accuracy using the first cycle is the worst (the SD reaches 0.1558) [Fig. 10(a)]. The prediction precision with 10% and half-life cycles is the second, with the SD of 0.1319 [Fig. 10(b)] and 0.1126 [Fig. 10(c)], respectively. The above analysis shows that when the SEDE model is used to calculate creep damage, the life-prediction accuracy of selecting characteristic cycle parameters as reference damage is also the highest. Additionally, the prediction accuracy for the SEDE model is better than that using the TF and DE models.

4. Evaluation based on the energy-life prediction model

In addition to the linear-damage-summation method, the inelastic-strain-energy could be used as a damage function to predict the fatigue life, which can characterize the internal damage of materials caused by cyclic deformation [54]. The application of this method in creep-fatigue deformation would be introduced as follows.

4.1. Evaluation based on the energy-life law

The relationship between the inelastic tensile strain energy (w_t) and the failure reversals $(2N_f)$ are as follows,

$$\mathbf{w}_{\mathsf{L}}(2\mathsf{N}_{\mathsf{f}})^{\mathsf{f}} = \mathsf{C} \tag{17}$$

The expression of w_t is,

$$\mathbf{w}_{t} = \frac{1 - \mathbf{n}'}{1 + \mathbf{n}'} \sigma_{T} \Delta \varepsilon_{in} \tag{18}$$

where n', σ_T , $\Delta\epsilon_{in}$, β , and C are the cyclic strain-hardening index, the maximum tensile stress, the inelastic strain, and the constants, respectively. The n' of the DZ445 superalloy is 0.2688 at 900 °C [52]. The statistical results of the inelastic-strain range and the maximum tensile stress with different cycles of the DZ445 superalloy at 900 °C could be obtained from our previous study [52].

Substituting the above data into Eqs.17 and 18, the relationship between W_t and $2N_f$ under different cycles is fitted and shown in Fig. 11. The fitting parameters and coefficients of determination (R^2) are also listed in the figure. There is the same trend between W_t and $2N_f$, and the prediction equation shows a good correlation. The correlation of fitting under the selected characteristic cycle is the highest, the R^2 is 0.9052. The prediction correlation under the first cycle is the lowest (the R^2 is 0.8359). The values for 10% life and half-life cycles are the second, the R^2 is 0.8719 and 0.8687, respectively. Fig. 11(a', b', c', and d') shows the relationship between the predicted and measured lives under different cycles in Fig. 11(a, b, c, and d). It is found that most data of the predicted life fall within 2 times of the scattering band. The standard deviations of the predicted and measured lives are the same as the corresponding fitting correlation trend between W_t and $2N_f$ in Fig. 11(a, b, c and d). That is, the life accuracy of prediction under the selected characteristic cycle is the highest (the SD = 0.1965). The worst precision is in the first cycle (the SD = 0.2685), followed by 10%-life and half-life cycles, with the SD being 0.2325 and 0.2356, respectively.

4.2. Evaluation of modified energy-life law based on damage mechanisms

According to the research results in our previous study [55], the modified energy-life prediction model based on the damage mechanism were used to predict the creep-fatigue cyclic-life of the DZ445 superalloy [55],

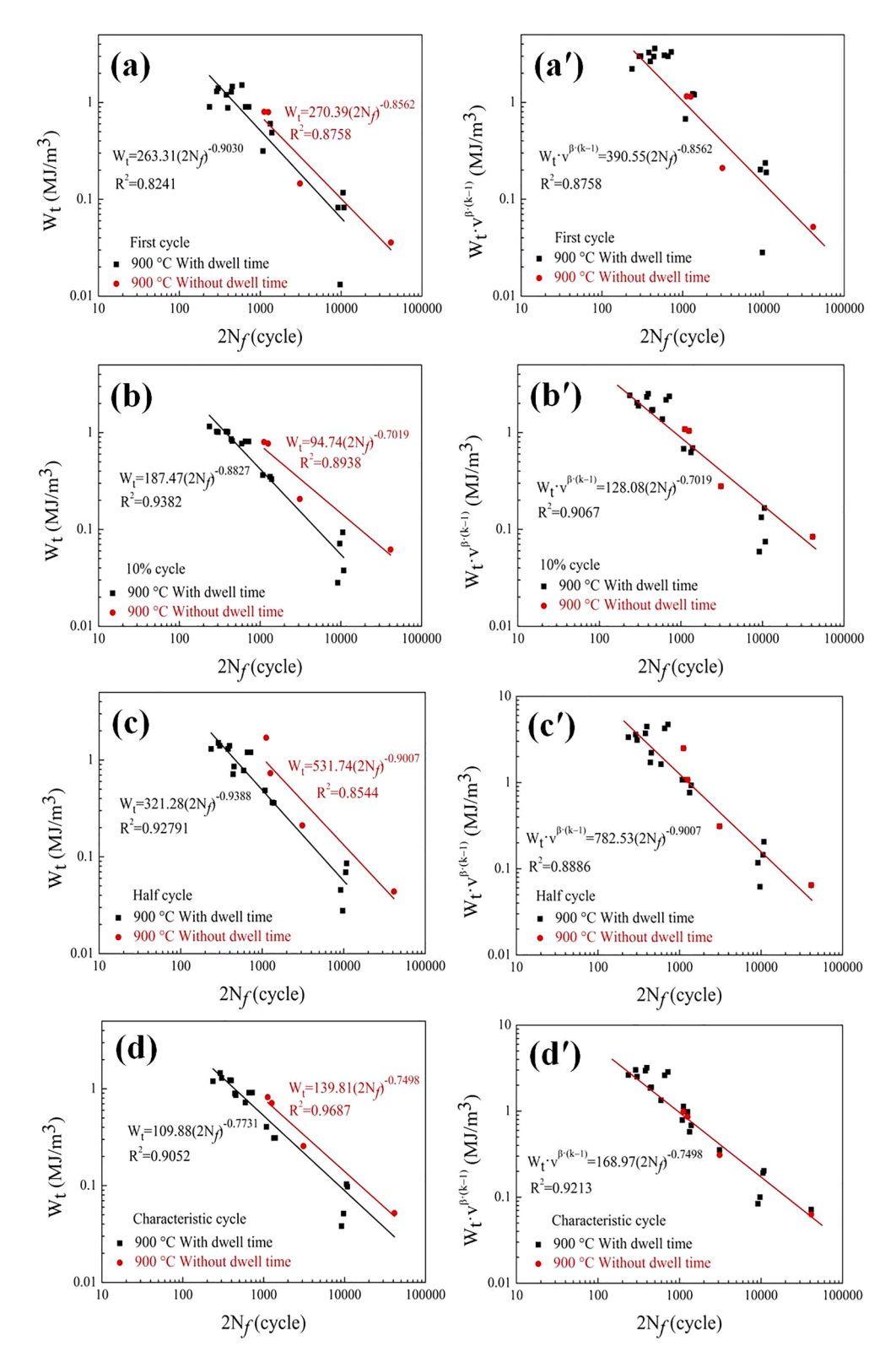


Fig. 13. Uncorrected (a, b, c, and d) and frequency corrected (a', b', c', and d') energy and as a function of cyclic life at $900 \,^{\circ}$ C for the DZ445 superalloy of creep-fatigue tests (a and a') the first; (b and b') the 10%-life; (c and c') the half-life; (d and d') the characteristic cycle.

$$W_{m} = 2/3 \left(\frac{1-n}{1+n} \sigma_{t,max} \Delta \varepsilon_{p,DE} + \frac{\sigma_{0}^{2} - \sigma(t)^{2}}{2E} \right) + 1/3 \left(2\frac{1-n}{1+n} K' \psi(t_{h}) \left(\frac{\Delta \varepsilon_{p,BE}}{2} \right)^{n'+1} = C_{m} \left(2N_{f} \right)^{-\beta_{m}}$$
(19)

the calculation method of the parameters in this formula is given in Reference [56]. The creep-fatigue data of the DZ445 superalloy comes from our previous experimental results [26,27].

The fitting relationship between the modified energy (W_m) and fatigue life of the DZ445 superalloy at different cycles and 900 °C is shown in Fig. 12(a, b, c and d). The R^2 between W_m and $2N_f$ are 0.9245, 0.8525, 0.9151, and 0.9193 with the first cycle, the 10%-life, the half-life, and the characteristic cycle, respectively. That is, the life prediction accuracy based on the characteristic cycle parameters is the highest, and that of the first cycle is the worst. The life-prediction accuracy after corrections is higher than that before modification. The errors between the measured and predicted lives under different cycles all fall within the 1.5–2 times scattering band [Fig. 12(a', b', c', and d')]. The prediction accuracy of the parameter under the selected characteristic cycle is the highest (SD = 0.1736), and that of the first cycle is the worst (SD = 0.2512). The precision of predictions at 10%-life and half-life cycles are the second, and the corresponding SD is 0.1829 and 0.1801, respectively.

4.3. Evaluation based on the frequency-corrected energy-life law

In the energy-based life-prediction models, there is also a kind method of the frequency correction. The deviation between the fitting line of creep-fatigue data with dwell time and pure fatigue data may because the influence of the related damage caused by oxidation on the cyclic life is not calculated in Eq. (16) [Fig. 13(a, b, c and d)]. The contribution of oxidation factors to the failure of alloy with dwell time cannot be ignored [57]. We need to add the frequency correction term, $V^{(k-1)}$, in Eq. (16) to introduce the influence of oxidation. Hence, all the corrected data points fall on a straight line as much as possible. The relationship between the frequency-correction energy (W_t) and $2N_f$ is expressed as [44],

$$W_{t}(2N_{f}V^{(k-1)})^{\beta} = C_{2}$$
(20)

where k and C₂ are the constants of the material, and V is the cyclic frequency in Hz,

$$V = \frac{1}{T_c + T_b} \tag{21}$$

where T_c and T_h are the dwell time introduced by a single cycle in pure low-cycle fatigue and creep-fatigue, respectively. The frequency of creep-fatigue under different dwell times is presented in Table 5.

Comparing with the Eqs. (17) and (20), the β value before and after the correction are found to be the same. By calculating the creep-fatigue data under different loading conditions, k=0.83 is obtained in the frequency-correction term. The value is then substituted into Eq. (20). The frequency-corrected energy (W_t) as a function of cyclic life (2N_f) at 900 °C for the DZ445 superalloy under the first cycle, the 10%-life, the half-life, and the characteristic cycles are shown in Fig. 13(a', b', c', and d'). The fitting equation and determination coefficient are also shown in this figure. Most of the data points with or without dwell time conform to the same linear relationship. Based on the characteristic-cycle data, the degree of correlation between the frequency-corrected W_t and 2N_f is the highest (R² is 0.9213). The R² is 0.8758, 0.9067, and 0.8886 at the first cycle, the 10%-life, and the half life cycles, respectively. They are all higher than the uncorrected determination coefficient between W_t and 2N_f in the corresponding cycle of Fig. 13(a, b, c, and d).

The cyclic life is predicted, based on the mechanical-response data under different creep-fatigue conditions at 900 °C. In the creep-fatigue deformation, the inelastic strain range ($\Delta \varepsilon_{in}$) consists of the plastic strain range ($\Delta \varepsilon_{pp}$) and the creep strain range ($\Delta \varepsilon_{cp}$) constitute, that is,

$$\Delta \varepsilon_{\rm in} = \Delta \varepsilon_{\rm pp} + \Delta \varepsilon_{\rm cp}$$
 (22)

according to Eq. (8), the stress value at any time during the relaxation-process can be obtained. The corresponding stress value at the end of the dwell-period could also be estimated. The stress value at the beginning of the dwell period could be approximated by the maximum tensile stress in the pure low-cycle fatigue test under the same total strain-range. Thus, the relaxed stress ($\Delta \sigma_r$) during the dwell-period can be estimated. The creep-strain range component ($\Delta \varepsilon_{cp}$) is,

$$\Delta \varepsilon_{\rm cp} = \Delta \sigma_{\rm r} / {
m E}$$
 (23)

where E is the elasticity modulus, and $\Delta \varepsilon_{pp}$ can be obtained by a pure low-cycle fatigue test. Based on this arrangement, the inelastic tensile strain energy with dwell time can be estimated. Therefore, the creep-fatigue cyclic life would be predicted according to Eqs. (6)–(20).

Table 5
Loading frequency with different dwell times in the creep-fatigue deformation.

D _t (s)	0	120	180	300	480	960	1920	3840	7680
V	0.08	0.0079	0.0054	0.0033	0.0021	0.0010	0.0006	0.0003	0.0001

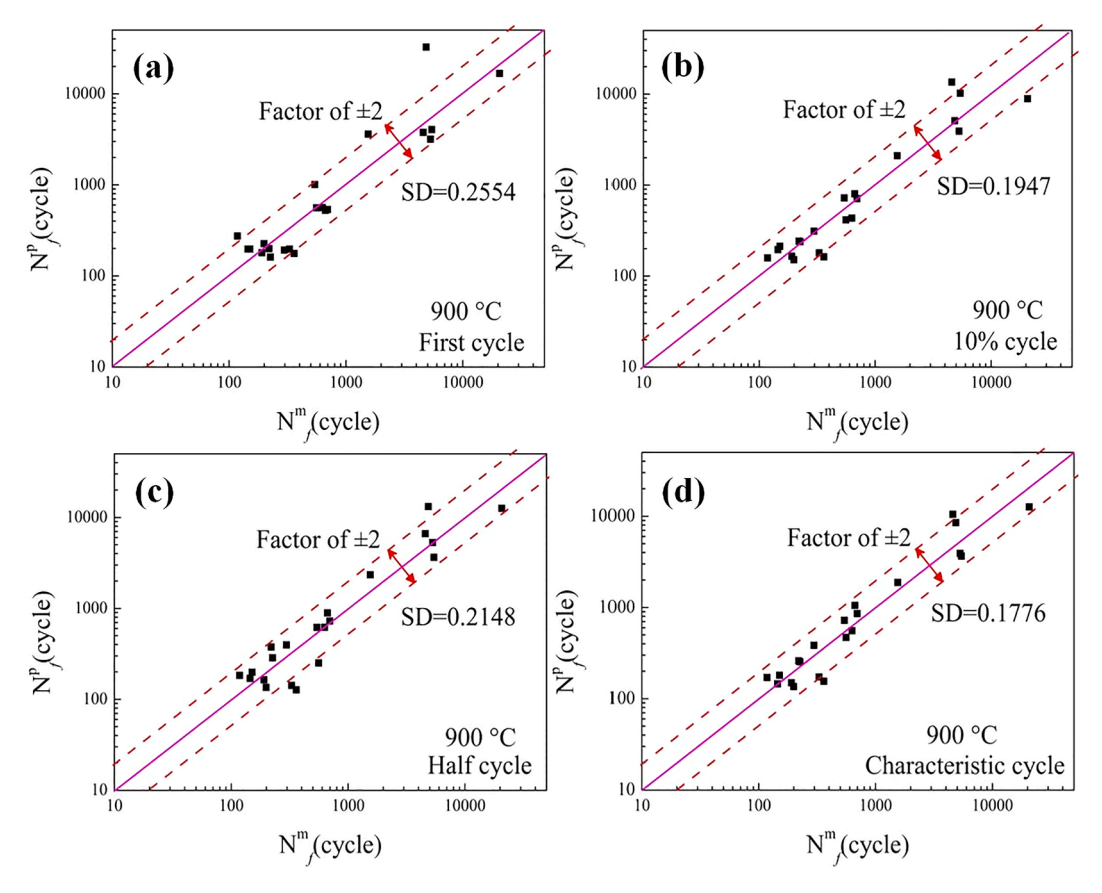


Fig. 14. Measured life (N_f^p) and predicted life (N_f^p) by the frequency-modified inelastic-strain energy method for the DZ445 superalloy at 900 °C of creep-fatigues (a) the first; (b) the 10%-life; (c) the characteristic; (d) the half-life cycles.

Based on the parameters of the first cycle, the 10%-life, the half-life, and the characteristic cycles, most of the deviations between the predicted and measured lives using the frequency-correction energy method fall within the 2-times line [Fig. 14(a, b, c, and d)]. The predicted accuracy by selecting characteristic cycle parameter is the best (SD is 0.1776). The forecasting accuracy for the first cycle is the worst (SD is 0.2554), followed by the value at 10%-life and half- life cycles, with the SD of 0.1947 and 0.2148, respectively. They are all higher than the prediction accuracy without any frequency correction [Fig. 11(a, b, c, and d)], indicating that the frequency-corrected energy could be used as the damage function to predict the creep-fatigue life well.

5. Discussion of the obtained results

5.1. Comparison of prediction accuracy in the parameters of different cycles

The linear-damage-summation and energy-based life rules are used to predict the creep-fatigue life in this investigation. We compared the prediction accuracy calculated by the parameters at the characteristic cycle, the first cycle, the 10%-life cycle, and the half-life cycle in both two models. It is found that the accuracy of life-prediction based on characteristic-cycle parameter with clear physical meaning is the highest (Figs. 7–14). The prediction precision of 10% life and half-life cycle is slightly second. This is because with the development of deformation, the plastic strain range at each cycle continues to increase [32,33]. Therefore, compared with the 10% life, the half-life, and the characteristic cycle, the plastic strain range under the first cycle is the smallest. Thus, the calculated inelastic strain rate is also the smallest with first cycle. The corresponding fracture elongation is large. Thus, the creep damage is small, resulting in the large predicted life. In our study, the stress responses at 10%-life and half-life cycles are similar. Thus, their life-prediction accuracies are similar. However, the characteristic cycle is defined as the "turning point" between the initial rapid-softening and the subsequent slight-softening/hardening of the maximum tensile stress, which represents the transition from the unstable-state (the rapid generation of dislocations) to the steady-state (the dynamic equilibrium of the generation and annihilation of dislocations) during deformation. The parameter with the highest prediction accuracy at the characteristic cycle may be related to the movement of the dislocation and the change of the microstructure during creep-fatigue deformation, which needs to be further studied in the future. This investigation provides a new creep-fatigue life-prediction method both in laboratory experiment and engineering components, which is convenient and accurate.

5.2. Comparison of prediction accuracy in the evaluation of different creep damage in LDS

The linear-damage-accumulation model has clear physical significance and simple operation [58,59]. In the linear-damage-summation rule, the fatigue damage is usually calculated by traditional-parameter method of Coffin-Manson law [60]. The time-fractional model is used to calculate the creep-damage whose deviation between the predicted and measured life is 3 times (Fig. 7). The advantage of this model is that the expression form is simple and only fewer standard experiments are needed to determine the parameters [61]. However, it does not consider the damage caused by the interaction between creep and fatigue. Only a simple accumulation of fatigue and creep damage is made in this model. In practice, the interaction between creep and fatigue cannot be ignored. The life calculated by this method is often conservative, mainly because the mutual damage is not considered. Therefore, this method is not suitable for the design and the life prediction of some important and precision components [61].

When calculating the creep-damage using the simple ductility-exhaustion model, all the predicted creep-fatigue cyclic-life is within the scattering factor of 2 times (Fig. 9). However, the application of this model to predict creep-damage is sometimes over-evaluated, resulting in the short predicted life [24]. In this model, the damage caused by creep and fatigue is described separately. The damage caused by the conditions that have a great impact on the interaction is not considered. This method is suitable for the life prediction of materials under the condition of single damage dominated by creep or fatigue [62].

Compared with the simple ductility-exhaustion model, the strain-energy-density-exhaustion model gives a more reasonable prediction result, whose predicted life deviation is 1.5 times (Fig. 10). The model considers the influence of two factors for the stress and the strain parameters, and has higher prediction accuracy [54]. However, the main disadvantage of this model is that more standard experiments are required to determine the parameters in the model. Zhang [63] believes that the model may produce more conservative results for the predicted life under a lower total strain-range. Zhu [64] once modified the calculation of the inelastic-strain energy part of this model to improve the life-prediction accuracy. According to the evolution of the damage parameters (plastic strain range, peak stress, and plastic-strain-energy-density) in 429EM stainless steel, the change of plastic-strain-energy-density in the whole fatigue process is relatively small. Therefore, it is best to use the plastic-strain-energy as the damage parameter for life prediction [65]. In general, the life-prediction accuracy of the creep-damage based on the time-fraction, the simple ductility-exhaustion, and the strain-energy-density exhaustion model is sequentially improved in the linear-damage-summation rule.

5.3. Comparison of prediction accuracy in the evaluation of different energy-life laws

In creep-fatigue deformation, the material will gradually consume a certain amount of energy. The more accumulated damage results in the more dissipated energy. Once the critical energy is reached, the fracture occurs [66]. Under the cyclic load, the movement of dislocation is described by cyclic plastic strain, and the resistance of its movement is described by cyclic stress. The plastic strain energy of comprehensive stress and strain parameters under each cycle is considered to be a measure of creep-fatigue damage under this cycle [67]. Therefore, the energy perspective can be used to quantify this relationship [68]. Under high temperature creep-fatigue deformation, researchers use energy parameters to evaluate the life of materials under different loading conditions through the hysteresis loop [26]. These methods are usually called as the energy-based life prediction models. However, most of these models ignore the effect of mean strain or stress in creep-fatigue on fatigue life [48]. For example, the prediction accuracy deviation of energy-life model shown in Fig. 11 is relatively large. In general, the accuracy of energy-based life prediction model needs to be further improved.

Many studies believe that the area of tensile stress in hysteresis loop is the driving force for fatigue crack initiation and propagation [54,68–71]. Shi [25] selected the total area of hysteresis loop as the measure of material damage. It is considered that the contribution of tensile and compressive stress to material damage is equivalent. Since the elastic deformation can be recovered, the plastic deformation will lead to the accumulation of material damage. Thus, Zhu [72] believed that the area above the elastic-plastic intersection of the tensile part should be selected as the damage measure. We reviewed the expression of energy-based life model: $w \cdot (2N_T)^{\beta} = C$. We found that the selection of damage (W) is phenomenological. In essence, the exponent of β and constant of C are only the parameter in the fitted expression. They cannot reflect the contribution of tensile and compressive stresses to cyclic damage in creep-fatigue deformation. Compared with the unmodified energy-life model, as shown in Fig. 12, we found that after the creep-fatigue life prediction model modified based on the tensile- and compressive- stress damage mechanism, the life prediction accuracy was improved [55].

Based on the energy principle, some attempts have been made to explain the effects of creep and mean strain/stress in life prediction. However, the applicability of these models was found to be limited because the time-dependent factors of creep/oxidation were not fully considered in these models. The damage model based on creep-fatigue-oxidation has also been tried to reveal by researchers [73–76]. In the energy-life prediction model modified by frequency factor (as shown in Fig. 13) [77], the life prediction accuracy is also improved. In summary, compared with the linear-damage-accumulation rule, the life-prediction model based on energy can not only take into account the prediction accuracy, but also has clear physical significance. The overall life prediction accuracy is also greater than that of LDS rule.

5.4. Summary and comparison of different life prediction models

In order to better compare the advantages and limitations of different creep-fatigue life predictions, we summarize the advantage and disadvantages of each life-prediction model in a separate Table 6.

 Table 6

 The advantage and disadvantages of each creep-fatigue life-prediction model.

Models/Test conditions	Time-fraction	Simple ductility-exhaustion	Strain-energy-density exhaustion	Energy-life	Damage mechanisms- correction	Frequency-correction
Advantages	Simple form and few parameters are required	Improved prediction accuracy	Clear physical meaning and improved prediction accuracy	Considering physical mechanism and prediction accuracy	Considering contributions of tensile and compressive stress to damage	Considering time factor related to oxidation and creep damage
Disadvantages	Negligence of interaction between creep and fatigue and poor prediction accuracy	Negligence of interaction between creep and fatigue and more standard experiments are needed	Negligence of interaction between creep and fatigue and more standard experiments are needed	Negligence of oxidation and mean stress	More standard experiments are needed to determine the required parameters	More standard experiments are needed to determine the required parameters
Scope of application	Simple life- prediction of non- important and non-precision parts	Creep or fatigue single damage- dominated	Accurate life prediction of important components	Little influence of mean stress and oxidation	Obvious mean stress	Long dwell and experiment time

6. Conclusions

The creep-fatigue data of the DZ445 superalloy at $900\,^{\circ}$ C are introduced in this manuscript. Compared the characteristic cycle, the first cycle, the 10%-life, and the half-life cycles parameters are applied to the linear-damage-summation rule and the energy-based life prediction model, respectively. The parameter with the highest prediction accuracy at the characteristic cycle may be related to the movement of the dislocation and the change of the microstructure during creep-fatigue deformation, which needs to be further studied in the future. Some conclusions could be found as follow:

- (1) The optimal critical-value of fatigue and creep damage in the linear-damage-summation method, that is, the coordinates of the intersection of the creep-fatigue envelope are determined. Compared with the coordinates of (0.5, 0.5), (0.3, 0.3), and (0.1, 0.01), there is the highest life prediction accuracy with the value of (0.1, 0.1).
- (2) To evaluate the accuracy of predicted life by the linear-damage-summation method and energy-life model, it is obtained that the prediction accuracy of parameters at the characteristic cycle with clear physical meaning is the highest. The accuracy of predication based on first cycle is the worst, and that for the 10%-life cycle as well as the half-life cycle are the second.
- (3) In the linear-damage-summation rule, the life-prediction accuracy of the creep- damage based on the time-fraction, the simple ductility-exhaustion, and the strain-energy-density exhaustion model is sequentially improved.
- (4) The life-prediction accuracy based on damage mechanisms and frequency-correction energy is higher than the value without any correction.

Declaration of Competing Interest

The authors declare that they have no known competing financial interests or personal relationships that could have appeared to influence the work reported in this paper.

Acknowledgments

W.L.R. is grateful for financial supports from the National Science Foundation of China (NSFC) (Grant number 51871142), the Independent Research and Development Project of State Key Laboratory of Advanced Special Steel, Shanghai Key Laboratory of Advanced Ferrometallurgy, Shanghai University (SKLASS 2020-Z04) and the Science and Technology Commission of Shanghai Municipality (No. 19DZ2270200). B.D. is grateful for the financial support from the fellowship of China Postdoctoral Science Foundation (2021M692020). Y.B.Z. is grateful for the financial support from the National Key Research and Development Program of China (2018YFF0109404, 2016YFB0300401, and 2016YFB0301401), the National Natural Science Foundation of China (U1732276 and U1860202). P. K. L. very much appreciates the supports from the National Science Foundation (DMR-1611180 and 1809640) with the program directors, Drs. Judith Yang, Gary Shiflet, and Diana Farkas.

References

- [1] Zhang XC, Gong JG, Xuan ZF. A deep learning based life prediction method for components under creep, fatigue and creep-fatigue conditions. Int J Fatigue
- [2] Ge L, Jiang W, Wang Y, Tu ST. Creep-fatigue strength design of plate-fin heat exchanger by a homogeneous method. Int J Mech Sci 2018;146:221–33.
- [3] Riedel H, Maier G, Oesterlin H. A lifetime model for creep-fatigue interaction with applications to the creep resistant steel P92. Int J Fatigue 2021;150:106308.
- [4] Zhu SP, Yang YJ, Huang HZ, Lv Z, Wang HK. A unified criterion for fatigue-creep life prediction of high temperature components. Proc Inst Mech Eng Part G: J Aerosp Eng 2017;231(4):677–88.
- [5] Wöhler A. Theorie rechteckiger eiserner Brückenbalken mit Gitterwänden und mit Blechwänden. Zeitschrift für Bauwesen 1855;5:121–66.
- [6] Basquin O. The exponential law of endurance tests. Proc Am Soc Test Mater 1910;10:625-30.
- [7] Coffin Jr LF. A study of the effects of cyclic thermal stresses on a ductile metal, trans. Am Soc Mech Eng 1954;76:931–50.
- [8] Manson SS. Behavior of materials under conditions of thermal stress. Natl Advisory Committ Aeronaut 1954:145-7.
- [9] Halford GR. Evolution of creep-fatigue life prediction models. Creep-Fatigue Interact High Temp 1991:43-57.
- [10] Chen X, Fan Z, Chen L, Jiang J, Yang T. Discussion of several life prediction methods for fatigue-creep interaction. International Fracture Mechanics Conference. 2007.
- [11] Korsunsky AM, Dini D, Dunne FPE, Walsh MJ. Comparative assessment of dissipated energy and other fatigue criteria. Int J Fatigue 2007;29:1990-5.
- [12] Sabour MH, Bhat RB. Lifetime prediction in creep-fatigue environment. Mater Sci Poland 2008;26:563-84.
- [13] Takahashi Y, Dogan B, Gandy D. Systematic Evaluation of Creep-Fatigue Life Prediction Methods for Various Alloys. In: ASME 2009 Pressure Vessels and Piping Conference; 2009. p. 1461–70.
- [14] Zhang G, Yuan H, Li F. Analysis of creep-fatigue life prediction models for nickel-based superalloys. Comput Mater Sci 2012;57:80–8.
- [15] Yan XL, Zhang XC, Tu ST, Mannan SL, Xuan FZ, Lin YC. Review of creep-fatigue endurance and life prediction of 316 stainless steels. Int J Press Vessels Pip 2015; 126:17–28.
- [16] Zhang XC, Tu ST, Xuan F. Creep-fatigue endurance of 304 stainless steels. Theor Appl Fract Mech 2014;71:51-66.
- [17] Wong EH, van Driel WD, Dasgupta A, Pecht M. Creep fatigue models of solder joints: A critical review. Microelectron Reliab 2016;59:1-12.
- [18] Yan XL, Zhang XC, Tu ST, Mannan SL, Xuan FZ, Lin YC. Review of creep-fatigue endurance and life prediction of 316 stainless steels. Int J Press Vessels Pip 2015;1262015:17–28.
- [19] Zhu SP, Huang HZ, Liu Y, He L, Meng D. A new ductility criterion for fatigue-creep life prediction of high temperature components. In: 55th AIAA/ASMe/ASCE/AHS/SC Structures, Structural Dynamics, and Materials Conference; 2014. p. 1058.
- [20] Payten WM, Dean DW, Snowden KU. A strain energy density method for the prediction of creep–fatigue damage in high temperature components. Mater Sci Eng A 2010;527(7–8):1920–5.
- [21] Priest RH, Ellison EG. A combined deformation map-ductility exhaustion approach to creep-fatigue analysis. Mater Sci Eng 1981;49:7–17.
- [22] Takahashi Y. Study on creep-fatigue evaluation procedures for high chromium steels-Part II: Sensitivity to calculated deformation. Int J Press Vessels Pip 2008; 85(6):423–40.

- [23] Mao J, Li X, Wang D, Zhong F, Luo L, Bao S, et al. Experimental study on creep-fatigue behaviors of Chinese P92 steel with consideration of several important factors. Int J Fatigue 2021:142:105900.
- [24] Wang Q, Xu Z, Wang X. An efficient fatigue and creep-fatigue life prediction method by using the hysteresis energy density rate concept. Fatigue Fract Eng Mater Struct 2020;43(7):1529–40.
- [25] Fan YN, Shi HJ, Tokuda K. A generalized hysteresis energy method for fatigue and creep-fatigue life prediction of 316L(N). Mater Sci Eng A 2015;625:205–12.
- [26] Zhu SP, Huang HZ, He LP, Liu Y, Wang Z. A generalized energy-based fatigue-creep damage parameter for life prediction of turbine disk alloys. Eng Fract Mech 2012;90:89–100.
- [27] Campbell RD. Creep/fatigue interaction correlation for 304 stainless steel subjected to strain-controlled cycling with hold times at peak strain. J Eng Ind 1971; 93:887–95.
- [28] Alsmadi ZY, Alomari A, Kumar N, Murty KL. Effect of hold time on high temperature creep-fatigue behavior of Fe-25Ni-20Cr (wt.%) austenitic stainless steel (Alloy 709). Mater Sci Eng A 2020;771:138591.
- [29] Zhao L, Xu L, Han Y, Jing H. Analysis on stress-strain behavior and life prediction of P92 steel under creep-fatigue interaction conditions. Fatigue Fract Eng Mater Struct 2020;43(11):2731–43.
- [30] Takahashi Y. Study on creep-fatigue evaluation procedures for high-chromium steels-Part I: Test results and life prediction based on measured stress relaxation. Int J Press Vessels Pip 2008;85(6):406–22.
- [31] Chen X, Sokolov MA, Sham S, DLE III, Busby JT, Mo K, et al. Experimental and modeling results of creep-fatigue life of Inconel 617 and Haynes 230 at 850 °C 2013;432:94–101.
- [32] Wang RZ, Zhang XC, Gong JG, Zhu XM, Tu ST, Zhang CC. Creep-fatigue life prediction and interaction diagram in nickel-based GH4169 superalloy at 650 °C based on cycle-by-cycle concept. Int J Fatigue 2017;97:114–23.
- [33] Wang X, Zhang W, Gong J, Wahab MA. Low cycle fatigue and creep fatigue interaction behavior of 9Cr-0.5 Mo-1.8 WV-Nb heat-resistant steel at high temperature. J Nucl Mater 2018;505:73–84.
- [34] Wang RZ, Guo SJ, Chen H, Wen JF, Zhang XC, Tu ST. Multi-axial creep-fatigue life prediction considering history-dependent damage evolution: A new numerical procedure and experimental validation. J Mech Phys Solids 2019;131:313–36.
- [35] Ding B, Ren W, Zhong Y, Yuan X, Peng J, Zheng T, et al. Analysis of the fully-reversed creep-fatigue behavior with tensile-dwell periods of superalloy DZ445 at 900 °C. Eng Fract Mech 2021;250:107781.
- [36] Ding B, Ren W, Deng K, Li H, Liang Y. An abnormal increase of fatigue life with dwell time during creep-fatigue deformation for directionally solidified Ni-based superalloy DZ445. High Temp Mater Processes (London) 2018;37(3):277–84.
- [37] Ding B, Ren W, Peng J, Zhong Y, Yu J. Influence of dwell time on the creep-fatigue behavior of a directionally solidified Ni-based superalloy DZ445 at 850 °C. Mater Sci Eng A 2018;725:319–28.
- [38] Taira S. Lifetime of structures subjected to varying load and temperature, Creep in structures. Berlin, Heidelberg: Springer; 1962. p. 96-124.
- [39] Code A. American Society of Mechanical Engineers Boiler and Pressure Vessel Code, Appendix G to Part. 1980;12:123-32.
- [40] Code RM. Design and Constriction Rules for Mechanical Components of FBR Nuclear Islands, appendix A16 2007;45:345-56.
- [41] Skelton R, Gandy D. Creep-fatigue damage accumulation and interaction diagram based on metallographic interpretation of mechanisms. Mater High Temp 2008:25:27–54.
- [42] Skelton R. Developments in creep-fatigue crack initiation and growth procedures in high temperature codes. Mech Behav Mater High Temp 1996;232:281–97.
- [43] Manson SS, Halford GR. Fatigue and Durability of Metals at High Temperatures. ASM Int 2009;9:114-21.
- [44] Goyal S, Mariappan K, Shankar V, Sandhya R, Laha K, Bhaduri AK. Studies on creep-fatigue interaction behaviour of Alloy 617M. Mater Sci Eng A 2018;730: 16–23.
- [45] Chang YJ, Bae JC, Kang CS, Cho JI, Son HT. Normalized creep-fatigue life prediction model based on the energy dissipation during hold time. Mater Sci Eng A 2007;460:195–203.
- [46] Takahashi Y, Shibamoto H, Inoue K. Study on creep-fatigue life prediction methods for low-carbon nitrogen-controlled 316 stainless steel (316FR). Nucl Eng Des 2008;238:322–35.
- [47] Wright J, Sham S. Creep-Fatigue Interaction Diagram for Alloy 617 in Air at 950 °C. Eng Calculat Anal Report 2010;35:1199-209.
- [48] Chen L, Wu W, Liaw PK. Creep-fatigue interaction behavior and life prediction of three kinds of superalloys. Acta Metall Sin 2006;42:952-8.
- [49] Wang Y, Dong J, Zhang M, Yao Z. Stress relaxation behavior and mechanism of AEREX350 and Waspaloy superalloys. Mater Sci Eng A 2016;678:10-22.
- [50] Goldhoff R. Uniaxial creep-rupture behavior of low-alloy steel under variable loading conditions. J Basic Eng 1965;87:374-8.
- [51] Teed PL. Creep and stress relaxation in metals. Edited by IA Oding. Oliver & Boyd, Edinburgh and London. Aeronaut J 1966;70:679.
- [52] Xu H. Study on Fatigue Properties of Directionally Solidified Nickel-Based Superalloy DZ445. Shenyang University of Technology; 2012.
- [53] Chaboche JL. Constitutive equations for cyclic plasticity and cyclic viscoplasticity. Int J Plast 1989;5:247-302.
- [54] Ostergren W. A damage function and associated failure equations for predicting hold time and frequency effects in elevated temperature, low cycle fatigue. J Test Eval 1976;4(5):327–39.
- [55] Ding B, Ren W, Peng J, Zheng T, Hou L, Yu J, et al. Damage mechanism and life prediction based on tensile-stress-and compressive-stress-dominated low-cycle fatigue of a directionally solidified Ni-based superalloy DZ445. Mater Sci Eng A 2019;742:478–92.
- [56] He ZZ, Zhang Y, Qiu W, Shi HJ, Gu J. Temperature effect on the low cycle fatigue behavior of a directionally solidified nickel-base superalloy. Mater Sci Eng A 2016;676:246–52.
- [57] François D, Pineau A, Zaoui A. Creep-fatigue-oxidation interactions. Mechanical Behaviour of Materials. Dordrecht: Springer; 2013. p. 407-81.
- [58] Tahir F. Creep-Fatigue Damage Investigation and Modeling of Alloy 617 at High Temperatures [Ph. D. Thesis]; 2017.
- [59] Chen LJ, Yao G, Tian JF, Wang ZG, Zhao HY. Fatigue and creep-fatigue behavior of a nickel-base superalloy at 850 °C. Int J Fatigue 1998;20(7):543-8.
- [60] Chen G, Zhang Y, Xu D, Lin Y, Chen X. Low cycle fatigue and creep-fatigue interaction behavior of nickel-base superalloy GH4169 at elevated temperature of 650 °C. Mater Sci Eng A 2016;655:175–82.
- [61] Zhang XF. Persistence and life prediction of different materials under interactive creep-fatigue conditions. East China University of Science and Technology; 2014.
- [62] Zamrik SY, Mirdamadi M, Davis DC. Ductility exhaustion criterion for biaxial fatigue-creep interaction in type 316 SS at 1150 deg F(621 deg C). In: Material Durability/Life Prediction Modeling. Materials for the 21st Century; 1994. p. 107–34.
- [63] Wang RZ, Zhang XC, Tu ST, Zhu SP, Zhang CC. A modified strain energy density exhaustion model for creep-fatigue life prediction. Int J Fatigue 2016;90:12–22.
- [64] Zhu SP, Yang YJ, Huang HZ, Lv Z, Wang HK. A unified criterion for fatigue-creep life prediction of high temperature components. Proc Inst Mech Eng Part G: J Aerosp Eng 2017;231:677–88.
- [65] Lee KO, Hong SG, Lee SB. A new energy-based fatigue damage parameter in life prediction of high-temperature structural materials. Mater Sci Eng A 2008;496 (1–2):471–7.
- [66] Nagae Y. Evaluation of creep-fatigue life based on fracture energy for modified 9Cr-1Mo steel. Mater Sci Eng A 2013;560:752-8.
- [67] J D. Morrow Cyclic plastic strain energy and fatigue of metals, Internal friction, damping, and cyclic plasticity. ASTM International; 1965.
- [68] Skelton RP. The energy density exhaustion method for assessing the creep-fatigue lives of specimens and components. Mater High Temp 2013;30(3):183-201.
- [69] Skelton R. Energy criterion for high temperature low cycle fatigue failure. Mater Sci Technol 1991;7(5):427-40.
- [70] Tian Y, Yu D, Zhao Z, Chen G, Chen X. Low cycle fatigue and creep-fatigue interaction behaviour of 2.25 Cr1MoV steel at elevated temperature. Mater High Temp 2016;33(1):75–84.
- [71] Chen LJ, Wang ZG, Yao G, Tian JF. An assessment of three creep-fatigue life prediction methods for nickel-based superalloy GH4049. Fatigue Fract Eng Mater Struct 2000;23(6):509–19.
- [72] Zhu SP, Huang HZ, He LP, Hou MJ, Zhou LW. Improved generalized strain energy damage function method for high temperature and low cycle fatigue creep. Acta Aeronaut Sinica 2011;32(8):1445–52.

- [73] Fournier B, Sauzay M, Caes C, Noblecourt M, Mottot M, Bougault A, et al. Creep-fatigue-oxidation interactions in a 9Cr–1Mo martensitic steel. Part III: Lifetime prediction. Int J Fatigue 2008;30(10-11):1797–812.
- [74] Wang RZ, Zhang XC, Tu ST, Zhang CC. The effects of inhomogeneous microstructure and loading waveform on creep-fatigue behaviour in a forged and precipitation hardened nickel-based superalloy. Int J Fatigue 2017;97:190–201.
- [75] Wang RZ, Zhu SP, Wang J, Zhang XC, Tu ST, Zhang CC. High temperature fatigue and creep-fatigue behaviors in a Ni-based superalloy: Damage mechanisms and life assessment. Int J Fatigue 2019;118:8–21.
- [76] Wang RZ, Zhu XM, Zhang XC, Tu ST, Gong JG, Zhang CC. A generalized strain energy density exhaustion model allowing for compressive hold effect. Int J Fatigue 2017;104:61–71.
- [77] Xu H, Zhang WW, Maile K. Life prediction of two rotor steels under creep-fatigue interaction at elevated temperature, Applied Mechanics and Materials. Trans Tech Publications Ltd 2014;470:581–4.